Antiviral Research 100 (2013) 399–406

Contents lists available at ScienceDirect

Antiviral Research

journal homepage: www.elsevier.com/locate/antiviral

Inhibition of influenza hemagglutinin with the antiviral inhibitor arbidol using a proteomics based approach and mass spectrometry

Zainab H. Nasser, Kavya Swaminathan, Patrick Müller, Kevin M. Downard *

School of Molecular Bioscience, University of Sydney, Sydney, Australia

ARTICLE INFO

Article history:
Received 23 July 2013
Revised 25 August 2013
Accepted 27 August 2013
Available online 4 September 2013

Keywords:
Hemagglutinin
Influenza virus
Antiviral inhibitor
Arbidol
Gel electrophoresis

ABSTRACT

A proteomics gel electrophoresis based approach has been applied to study the effect of arbidol on the proliferation of influenza virus *in vitro* through quantitation of hemagglutinin levels. An arbidol concentration of 20 μg/ml was required to achieve a 50% reduction in virus proliferation and hemagglutinin levels. The use of a MALDI mass spectrometry approach to study the binding of arbidol to influenza hemagglutinin revealed it bound solely to residues 104–120 of the HA2 subunit, a region known to contain an arbidol resistance mutation. Parallel molecular docking results revealed that this binding site was favoured in which the arbidol molecule binds in two possible orientations approximately 180° to one another at HA2 residues 118–123. The combined studies support the recognized potential of arbidol as an effective and targeted antiviral agent against the influenza virus.

1. Introduction

Influenza is caused by an RNA virus of the orthomyxoviridae family. Complications include pneumonia, secondary bacterial infections, and bronchiolitis. Its widespread occurrence, and usually non-life threatening nature, has led to a degree of complacency about its devastating health and economic impact potential. Seasonal epidemics are responsible for three to five million cases of infection and up to 500,000 deaths annually (Wilschut et al., 2006; World Health Organization, 2009). Pandemic outbreaks, usually associated with reassorted strains of the virus for which the community have little to no immunity, can result in millions of deaths (Barry, 2006; Kilbourne, 2006).

The influenza virus is an antigenically variable virus that eludes inactivation and detection through point mutations in the genes that encode the hemagglutinin and neuraminidase glycoproteins on the surface of the virus particle. This is compounded by antigenic shift where genes of the virus' segmented genome are interchanged or reassorted in a host cell infected with two or more strains (Pereira, 1980; Hampson and Mackenzie, 2006; Bouvier and Palese, 2008).

Efforts to respond to, prevent or treat influenza are based on two separate approaches (Couch, 2000): vaccines (Poland et al., 2001) and antiviral medications (Moscona, 2005; Von Itzstein and Thomson, 2009). An effective vaccination response requires that large sections of the community are inoculated with strains in circulation before a natural infection occurs. Increasingly, antiviral medications are relied upon to tackle the threat that the virus poses (Von Itzstein and Thomson, 2009). However, current second-generation antiviral inhibitors that target the neuraminidase antigen on the surface of the virus have become ever more ineffective with a rise in the number of resistant strains to these agents. Between 2008 and 2009, resistance to the most common antiviral inhibitor, oseltamivir, was reported among almost 99% of the seasonal H1N1 strains in Europe and North America found to contain a common H274Y mutation (Hauge et al., 2009; Moscona, 2009). By August 2010, a year after the emergence of the swine-originating influenza virus (so called swine flu) more than 300 of these pandemic strains were also reported to be resistant (World Health Organization, 2010).

These findings have led to efforts to design, develop and test new antiviral agents. Peramivir was approved for emergency use during the 2009 H1N1 pandemic outbreak (Birnkrant and Cox, 2009) but widespread oseltamivir resistance has reduced its potential (Hurt et al., 2009). The pro-drug laninamivir, a structural analogue of zanamivir, has been approved for use against influenza in some countries (Vavricka et al., 2011).

Arguably the ideal target of an antiviral agent to the influenza virus is the hemagglutinin surface glycoprotein. Although present in larger copy numbers than the neuraminidase, this protein plays a major role in initiating the viral replication. The hemagglutinin drives the attachment of the virus to the host cell by binding to cell-surface sialic acid receptors thereby mediating viral entry and infection (Fanning and Taubenberger, 1999; Gamblin et al.,

* Corresponding author. Address: School of Molecular Bioscience G-08, The University of Sydney, Sydney, NSW 2006, Australia. Tel.: +61 (0) 2 9351 4140.
E-mail address: k.downard@sydney.edu.au (K.M. Downard).

0166-3542/$ - see front matter © 2013 Elsevier B.V. All rights reserved.
http://dx.doi.org/10.1016/j.antiviral.2013.08.021

2004). The hemagglutinin glycoprotein represents a center of antigenic variation in influenza viruses and it is the principal component of the virus subject to immune selection (Subbarao and Katz, 2000).

Arbidol (Fig. 1) is a broad-spectrum antiviral drug that has been demonstrated to be active against various non-enveloped and enveloped viruses (Shi et al., 2007). This drug has been reported to be a potent prophylactic treatment of various respiratory infections including influenza. While approved for use in China and Russia it has not gained acceptance in western countries. It is believed to utilize a molecular mechanism against both type A and B influenza viruses that is different from other antivirals and involves inhibition of virus-mediated fusion to block viral entry into the host cell (Boriskin et al., 2008). Fusion requires that the hemagglutinin protein undergo conformational changes that occur only under acidic pH conditions. Such changes lead to the exposure of the N-terminal fusion peptide within the HA2 subunit and allow it to interact with the target endosomal membrane (Boriskin et al., 2008). Within 1 h of the pretreatment of MDCK cells with arbidol, yields of type A and B influenza virus were reduced by 70–80% (Boriskin et al., 2008).

To investigate the potential and mode of action of arbidol, we report here the application of gel electrophoresis to assess the ability of arbidol to inhibit the proliferation of influenza virus *in vitro*. These results are presented in parallel with an experimental molecular based MALDI-MS approach to study the mode of action of arbidol. This approach has recently been applied to study the binding of antiviral inhibitors to influenza neuramindase (Swaminathan and Downard, 2012; Swaminathan et al., 2013) and is based on an immunoassay developed earlier in this laboratory (Kiselar and Downard, 1999; Morrissey and Downard, 2006; Morrissey et al., 2007; Schwahn and Downard, 2009). The results are compared with those obtained computationally through the molecular docking of arbidol to influenza hemagglutinin.

2. Materials and methods

2.1. Vaccine and virus strains

A vaccine against the swine-originating influenza virus responsible for the 2009 pandemic was obtained from CSL Limited (Parkville, Victoria, Australia) and was used without further purification. It is an inactivated split virus vaccine that contains a A/California/7/2009-like strain and 30 μg/mL of hemagglutinin in solution. A recombinant hemagglutinin (full length HA0) based on the same strain was purchased from Sino Biologicals Inc. (Beijing, China). A human clinical specimen containing a post pandemic A/Brisbane/122/2011 (H1N1) strain was obtained from Mr. Robert Shaw and Dr. Ian Barr of the World Health Organization Collaborating Center for Influenza (Melbourne, Australia). It was passaged through MDCK cells before being precipitated and recovered.

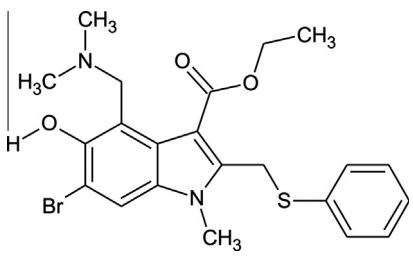

Fig. 1. Chemical structure of arbidol (or ethyl-6-bromo-4-[(dimethylamino)methyl]-5-hydroxy-1-methyl-2-[(phenylthio)methyl]-indole-3-carboxylate hydrochloride monohydrate). Molecular formula is $C_{22}H_{26}BrClN_2O_3S$ with mass of 513.88 (average).

2.2. Growth of clinical virus strain in cell culture with and without arbidol

Madin–Darby canine kidney (MDCK) cells were grown in complete Dulbecco's modified eagle medium (cDMEM) (Invitrogen, Victoria, Australia) supplemented with penicillin G (100 U/ml), streptomycin (100 μg/ml), 2 mM L-glutamine, 10% fetal bovine serum and 25 mM HEPES buffer.

The MDCK cells were washed twice with phosphate-buffered saline (PBS) solution (containing 0.137 M sodium chloride, 2.7 mM potassium chloride, 1.4 mM potassium dihydrogen phosphate and 0.01 mM disodium hydrogen phosphate in water) prior to being split. Trypsin/EDTA solution (3 ml at 0.25% (w/v)) was added and the cells incubated for 1–2 min at 37 °C. The detached cells were then resuspended in a 1:2–1:6 dilution and incubated overnight in 175.cm^2 flasks.

The cell monolayers were incubated with 0–40 μg/mL of arbidol in cDMEM for 30 min at 37 °C. The A/Brisbane/122/2011 clinical sample was diluted (1:10 v/v) in growth medium containing cDMEM with TPCK-trypsin (2 μg/ml) and added to all but one flask, a control containing only 40 μg/mL arbidol. The MDCK cells were inoculated with the diluted virus solution (3 mL) for 30 min at 37 °C and passaged once only. An additional 20 mL of growth medium was added and incubated at 37 °C for 2 days after which a 90% cytopathic effect was observed. The supernatant was centrifuged for 15 min at 300*g* at 4 °C. The clarified supernatant was transferred into a fresh tube and the virus was inactivated overnight at 37 °C with 0.02% formalin. The virus was then precipitated with 8% (w/v) of polyethylene glycol 6000 (PEG) overnight at 4 °C, recovered by centrifugation at 9500 RCF for 40 min and the pellet washed with 50 mM sodium bicarbonate (3 × 1 mL).

2.3. Deglycosylation of influenza hemagglutinin using N-glycosidase F

Deglycosylation of the hemagglutinin in the vaccine and clinical virus sample was performed to improve its separation from influenza nucleoprotein by SDS–PAGE (Li et al., 2010). The virus samples were first denatured in a solution containing 10% SDS and β-mercaptoethanol solution at 100 °C for 10 min. The denatured protein was allowed to cool and then centrifuged for 1 min at 3 RCF after which 10% Triton 100 (2.5 μL) was added. A solution of PNGase-F (250 units in 250 μL) (Roche Diagnostics, Sydney, Australia) was added and the combined solution incubated overnight at 37 °C.

2.4. SDS–PAGE for hemagglutinin quantitation

Solutions of the deglycosylated vaccine and recombinant HA were added to an equal volume of loading buffer comprised of 100 mM Tris–HCl at pH 6.8, 10% (v/v) glycerol, 2% (w/v) sodium dodecylsulphate and 3.3% (v/v) β-mercaptoethanol. Appropriate dilutions of the vaccine and virus samples were loaded on a polyacrylamide gel (12.5% separating, 5% stacking) so as to achieve the required loading of hemagglutinin (between 30–3000 ng) alongside a Precision Plus protein standard solution (15 μL) (Bio-Rad, Sydney, Australia). The cell grown virus was also added to loading buffer and loaded along side the standards. SDS–PAGE was performed with a Bio-Rad Powerpac 300 power supply (Bio-Rad, Hercules, CA, USA) at a constant of 200 V in a buffered solution made up of (25 mM) Tris at pH 7.5, (192 mM) glycine and 0.1% (w/v) SDS for 2 h. The separated bands were then visualized using a Sypro Ruby protein gel stain (Invitrogen, Melbourne, Australia). The gels were scanned using a Typhoon FLA9000 laser scanner (GE Healthcare, Sydney, Australia) and digitally stored.

2.5. Hemagglutinin band intensity analysis

The intensity of each hemagglutinin band was measured using ImageJ software (NIH, Maryland, USA) applying background correction. The band intensities derived from each common loading of protein in the vaccine and recombinant hemagglutinin samples were plotted to establish a linear correlation (Fig. 2). The equation for the line of best fit of ($y = 0.9989 \times -0.0229$; $R^2 = 0.9975$) was used to determine the amount of hemagglutin present in the cell cultured A/Brisbane/122/2011 strain samples treated with and without arbidol.

2.6. In-gel tryptic digestion of hemagglutinin

The hemagglutinin bands of the vaccine and recombinant protein solutions for the 3000 ng loadings, along with the hemagglutinin band of the arbidol free (0 μg/mL) cell cultured clinical sample were excised from the gel and reconstituted in acetonitrile (300 μL) and 100 mM NH_4HCO_3 (300 μL). They were washed with 100 mM NH_4HCO_3 containing 50% acetonitrile solution. The gel pieces were subsequently immersed in 10 mM dithiothreitol for 30 min at 60 °C and then 50 mM iodoacetamide at room temperature for 30 min. 100 mM NH_4HCO_3 followed by 20 mM NH_4HCO_3 in 50% acetonitrile was used to wash out the excess iodoacetamide after which the gel pieces were dried in a vacuum concentrator (Labconco Coporation, Kansas City, USA). In-gel digestion was achieved by adding 15 ng/μL of trypsin (Promega, CA, USA) in 40 mM NH_4HCO_3 containing 10% acetonitrile and incubating the solution overnight at 37 °C. The resultant peptides were extracted by repeated sonication in 50% acetonitrile containing 5% trifluoroacetic acid, dried in a vacuum concentrator and resuspended in 25 mM NH_4HCO_3 solution (10 μL).

2.7. High resolution MALDI mass spectrometry

Each hemaglutinin digest solution (2 μL) was diluted 1:4 with 5 mg/mL α-cyano-4-hydroxycinnamic acid in 60% acetonitrile containing 0.1% TFA. 1 μL of this solution was spotted onto a MALDI sample plate (MTP AnchorChip 400/384 TF, Bruker Daltonics, Billerica, USA). MALDI mass spectra were recorded in the positive ion mode on a 7T Bruker APEX-Qe instrument (Bruker Daltonics, Billerica, USA) as previously described (Swaminathan and Downard, 2012; Swaminathan et al., 2013).

2.8. Binding of arbidol to hemagglutinin and native electrophoresis

A solution containing 5 μg of recombinant hemagglutinin was treated with a solution of arbidol (128 μg/mL in 1% ethanol) to achieve a 1:5 M ratio and incubated at 37 °C for 3 h. Solutions containing the arbidol bound hemagglutinin and untreated hemagglutinin were each diluted to 20 μL with water and 5 μL of loading buffer containing 1 M Tris (at pH 8.6) and 20% glycerol was added. The samples were loaded into separate wells of a 3–8% Tris–Acetate gel (Invitrogen, Melbourne, Australia). An additional solution of untreated hemagglutinin was diluted in the native loading buffer solution containing 0.1% Bromophenol Blue in order to track the location of the protein in a separate lane. Electrophoresis was performed in an Invitrogen MiniCell tank at 150 V for 60 min as previously described (Swaminathan and Downard, 2012; Swaminathan et al., 2013). The blind excised arbidol-bound hemagglutinin and untreated hemagglutinin was subjected to proteolytic digestion and MALDI analysis. The reminder of the gel was then stained with the Coomassie Blue solution to ensure that the hemagglutinin recovery was complete.

2.9. Limited proteolysis of untreated and arbidol bound hemagglutinin

The excised gel sections of each sample were pulverized into 1 mm^3 sections, transferred into separate 0.6 mL tubes and washed with milli-Q filtered water (300 μL). The gel pieces were then partially dried in a Labconco Centrivap concentrator (Kansas City, USA). The semi-dried pieces were rehydrated in a 25 mM NH_4HCO_3 solution (pH 7.8) (20 μL) containing one of three site-specific proteases: sequencing-grade-modified trypsin (Promega Corporation, Sydney, Australia); Glu-C (Sigma Aldrich, Sydney, Australia) or chymotrypsin (Boehringer Mannheim GmbH, Germany) at an enzyme: protein ratio of ~1:30 and incubated overnight at 37 °C. The gel pieces were sonicated for 2 × 1 h with additional 25 mM ammonium bicarbonate buffer (50 μL, pH 7.8) with periodic cooling on ice and the solutions pooled. The peptides were reduced and alkylated in a similar manner to that described above except that 10 μM dithiotheritol and 10 μM iodoacetamide (Sigma–Aldrich, Sydney,

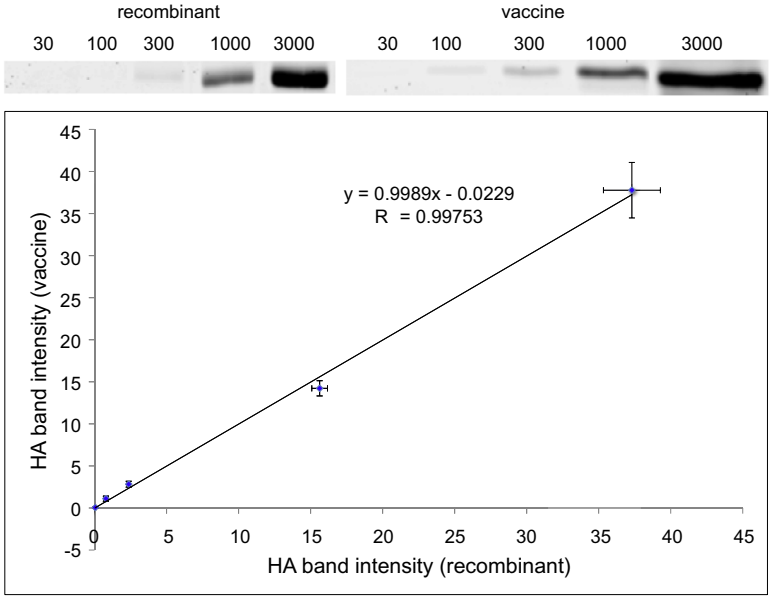

Fig. 2. Plot of the relative HA band intensity of the degylcosylated protein within a vaccine and recombinant protein solution across a range of loadings (30–3000 ng).

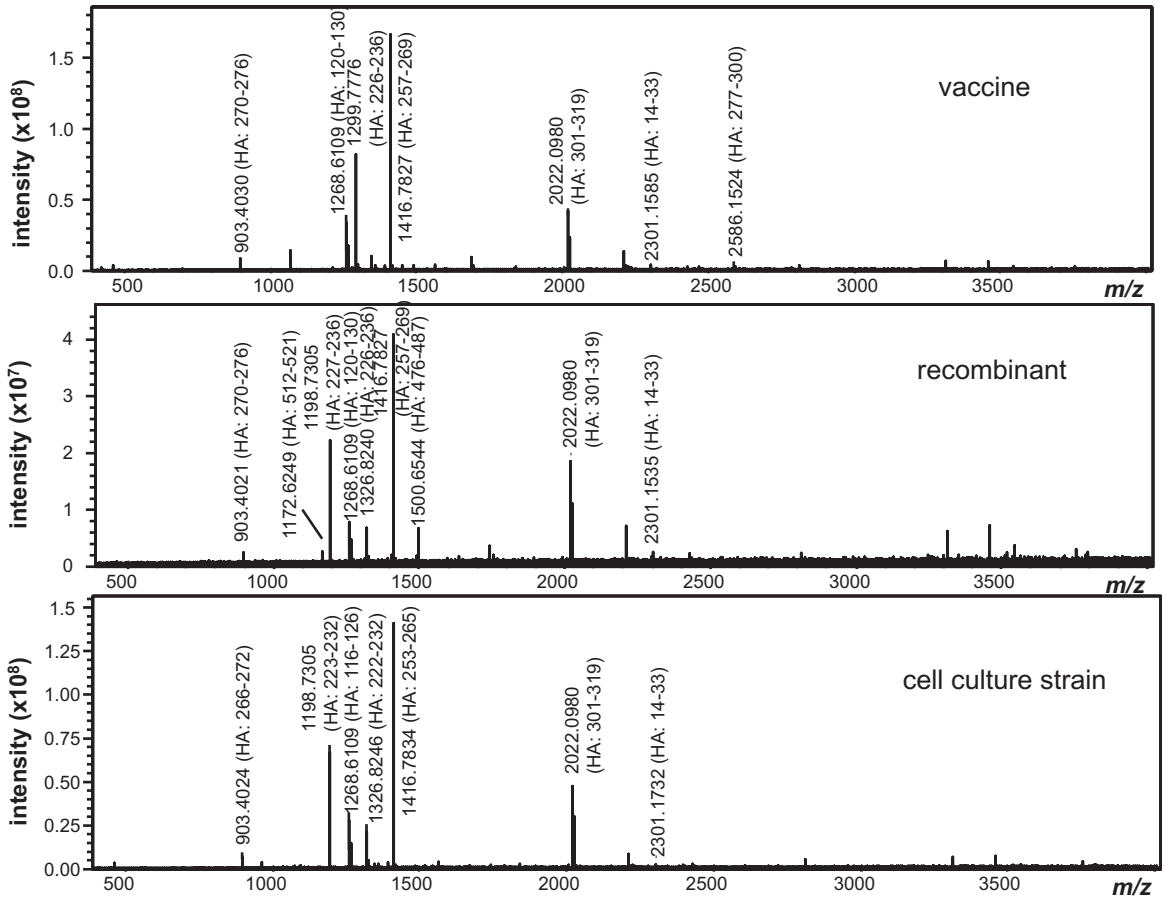

Fig. 3. MALDI mass spectra of the digested hemagglutinin band in each of the vaccine, recombinant protein and cell culture virus solutions.

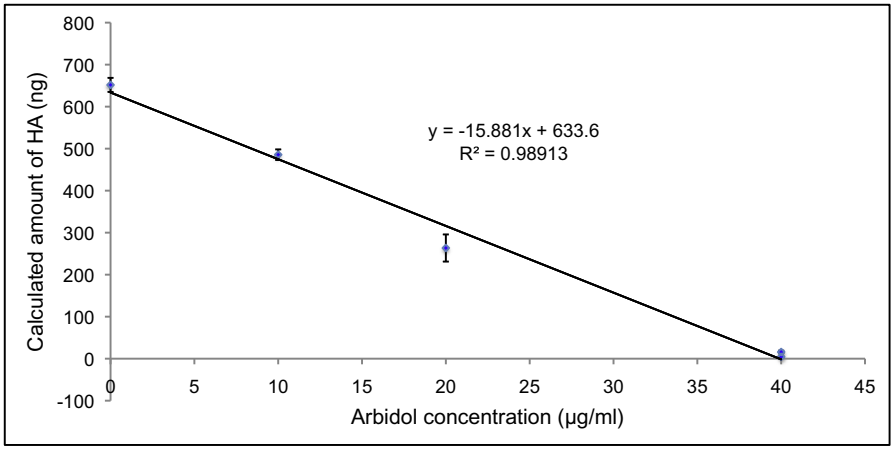

Fig. 4. Plot of the relative HA band intensity of the degylcosylated protein isolated from a cell cultured influenza virus (A/Brisbane/122/2011 H1N1) incubated with increasing concentrations of arbidol.

Australia) solutions were used. The final concentration of the peptides is expected to be 0.50 μg/μL, assuming 100% recovery.

2.10. Molecular docking of arbidol to influenza hemagglutinin

The arbidol structure was built using MarvinSketch software (ver. 5.12.3) (ChemAxon, Budapest, Hungary). The Xray crystal structure of the influenza hemagglutinin (PDB: 3LZG) was obtained for a H1N1 2009 pandemic strain (A/California/04/2009). Both the protein receptor and the ligand were prepared using the AutoDock program tools v1.5.4 and docked in two stages using AutoDock v4.2.3 (Scripps, La Jolla, USA). The first blind docking was performed using a cubic grid of 126 points at a resolution of 0.503 grid points per Å centered on and covering the HA2 subunit structure. A second, more focussed docking stage was centered on the identified binding site using a cubic grid of seventy points at a resolution of 0.375 points per Å. Docking was performed with the parameters ga_pop_size value of 150 and a ga_num_evals value of 10,000,000

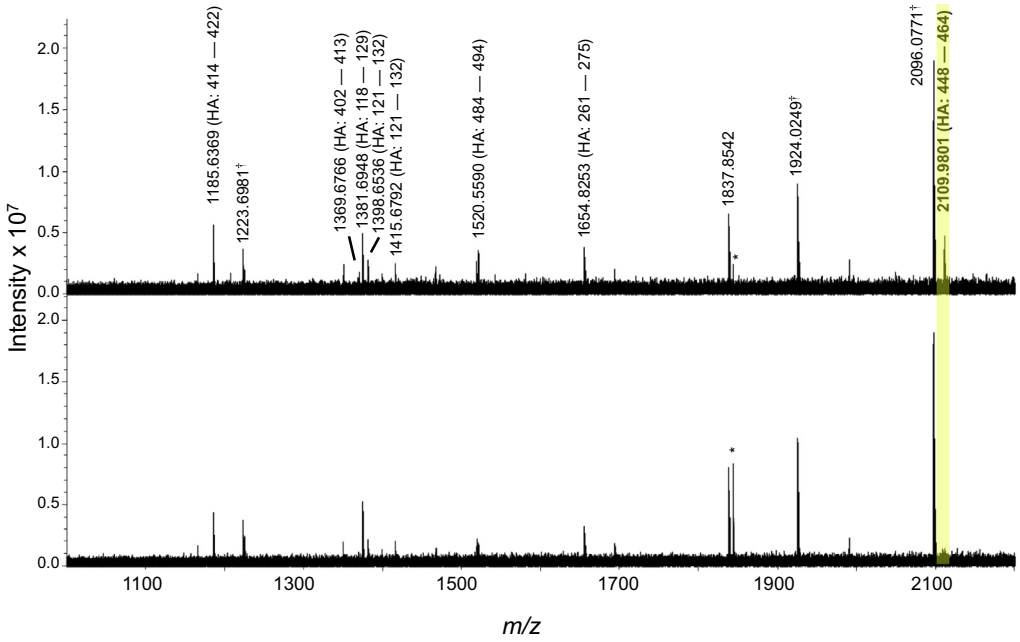

Fig. 5. MALDI mass spectra of recombinant hemagglutinin treated with and without arbidol before digestion with endoproteinase Glu-C. Ions denoted † and ∗ are autolysis products and those associated with background electronic noise respectively.

Table 1
Relative peak areas of Glu-C peptide ions produced from the digestion of recombinant hemagglutinin after treatment with and without arbidol. Values represent an average of duplicate data with standard deviations shown in brackets.

$[M+H]^+ m/z$ experimental	HA residues (HA0 numbering)	HA residues (HA2 numbering)	Sequence	Relative area without arbidol	Relative area with arbidol	Difference
545.3397	419–422	75–78	(E)KRIE	0.25 (0.07)	0.20 (0.00)	0.05 (0.07)
1185.6375	414–422	70–78	(E)FNHLEKRIE	9.95 (2.62)	6.30 (0.28)	3.65 (2.90)
1369.6777	402–413	58–69	(E)KMNTQFTAVGKE	1.75 (0.07)	1.70 (0.28)	0.05 (0.35)
1381.6959	118–129	–	(E)LREQLSSVSSFE	8.75 (1.49)	5.10 (1.27)	3.65 (0.21)
1398.6540	121–132	–	(E)QLSSVSSFERFE	3.25 (0.21)	2.00 (0.08)	1.25 (0.49)
1415.6799	121–132	–	(E)QLSSVSSFERFE	3.30 (0.57)	3.40 (0.28)	−0.10 (0.85)
1520.5597	484–494	140–150	(E)FYHKCDNTCME	8.55 (1.91)	4.60 (0.99)	3.95 (0.92)
1654.8258	261–275	–	(E)ATGNLVVPRYAFAME	13.90 (1.70)	8.35 (0.21)	5.55 (1.48)
2109.9801	448–464	104–120	(E)NERTLDYHDSNVKNLYE	15.25 (1.91)	3.45 (1.48)	11.80 (0.42)
2216.1758	382–401	38–57	(D)LKSTQNAIDEITNKVNSVIE	3.55 (1.77)	4.45 (0.35)	−0.90 (1.41)

with 250 conformations generated. These were clustered using an rmstol of 2.0 Å and processed with AutoDock. The results were visualized and prepared using the AutoDockTools program.

3. Results and discussion

3.1. Hemagglutinin quantitation with SDS–PAGE

The levels of hemagglutinin present within a proportion of a disrupted virus vaccine and recombinant protein solutions were analysed by measuring the band intensity of the deglycosylated protein resolved by SDS–PAGE (Fig. 2). This approach has been found to a reliable method to quantify hemagglutinin levels and produced results that are consistent with those obtained using a single radial immunodiffusion (SRID) method (Li et al., 2010). In accord, a direct linear correlation between the levels of hemagglutinin in the two sets of solution samples was found across several orders of magnitude ranging from 30–3000 ng of loaded protein. The band intensity measured in each case was background corrected through analysis of a portion of the gel without protein. An average value is plotted with errors shown for three replicate experiments (Fig. 2).

Fig. 2 demonstrates that the intensity of the hemagglutinin band is directly proportional to the amount of protein loaded. Thus the equation of the slope of the line can be used to determine the amount loaded in any unknown sample. Note that in each case the presence of hemagglutinin in the band was confirmed by MALDI-MS after in gel digestion of the protein with trypsin (Fig. 3). Each spectrum shares a similar set of ions consistent with a high degree of sequence homology in the hemagglutinin within the vaccine, recombinant protein and clinical specimen samples.

3.2. Inhibitory activity of arbidol on influenza virus growth

The plot shown in Fig. 2 enables levels of hemagglutinin to be quantified in the cell-cultured virus treated with different concentrations of the arbidol inhibitor. MDCK cells inoculated with varying concentrations of arbidol (from 0 to 40 μg/ml) were infected with the A/Brisbane/122/2011 H1N1 strain of the virus until a cytopathic effect was observed. A plaque assay determined the levels of virus to be 7×10^5 pfu/ml. The concentrations of antiviral used are below that found to induce a cytotoxic effect. A CC50 (50% cytotoxic concentration) value for arbidol has been reported to be between 40–60 μg/ml (Leneva et al., 1994).

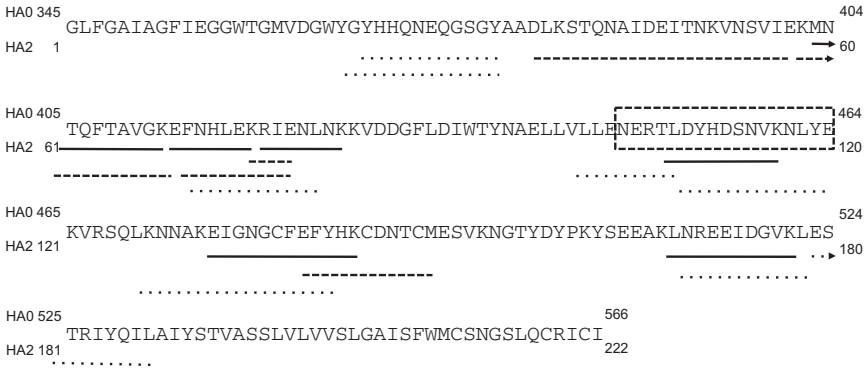

Fig. 6. Sequence of the hemagglutinin HA2 subunit showing the tryptic (—), chymotryptic (. . .) and endoproteinase Glu-C (—) peptides detected by MALDI-MS. Only the peptide segment boxed is found to bind to arbidol.

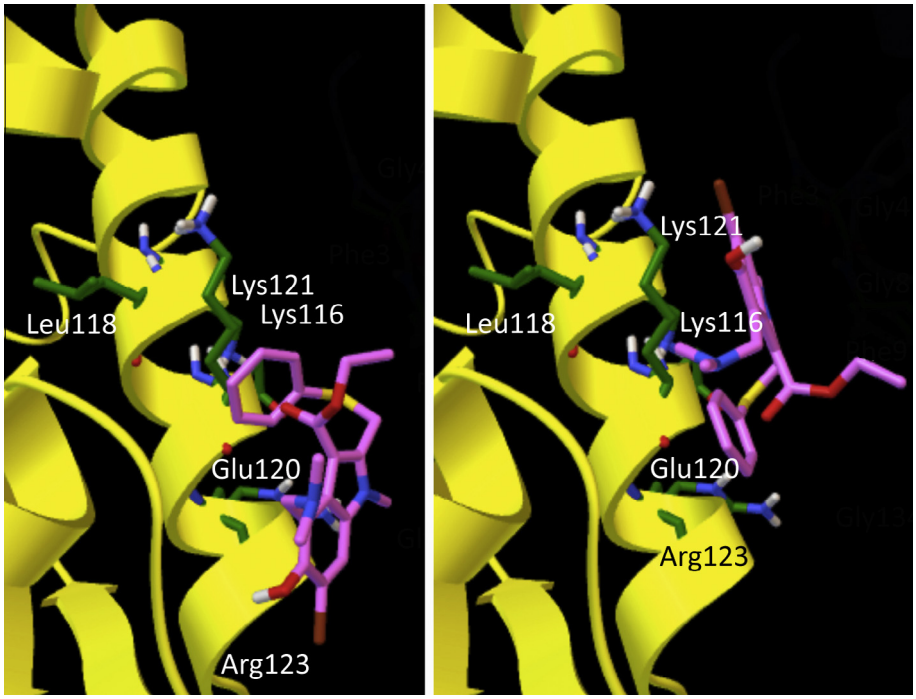

Fig. 7. Rank 1 (left) and rank 2 (right) from the results of the molecular docking of arbidol to the HA2 subunit of influenza hemagglutinin (3LZG). Note that part of some side chains of adjacent residues are also shown.

The virus in each of the cell cultured solutions was precipitated with polyethylene glycol and deglycosylated with PNGase F prior to analysis by SDS–PAGE (Fig. 4). A positive control sample that contained no arbidol and a negative control that contained no virus were also analysed. Using the plot shown in Fig. 2, the levels of hemagglutinin were determined from the band intensity to be between 652 ng and 0 ng with increasing arbidol concentrations from 0 to 40 μg/ml (Fig. 4). At 20 μg/ml the hemagglutinin levels decreased to 40.4%. From the slope of the line in Fig. 4, virus proliferation had reduced to about one half with this level of antiviral. The IC_{50} value was determined to be 17 ± 2 μg/ml by the percentage reduction method. The IC_{50} value for different strains of the influenza virus under various test conditions was found to be between 4 to 30 μg/ml consistent with this value (Boriskin et al., 2008) At 40 μg/ml, the virus was completely inhibited from replicating (Fig. 4). These gel based results clearly demonstrate the *in vitro* inhibitory activity of arbidol against the influenza virus.

3.3. Mode of action – binding of arbidol to influenza hemagglutinin by mass spectrometry

To investigate the mode of action of arbidol at the molecular level, the binding of arbidol to the hemagglutinin protein was studied employing a MALDI-MS based approach recently applied to study the binding of other antiviral inhibitors (Swaminathan and Downard, 2012; Swaminathan et al., 2013).

A solution of recombinant hemagglutinin representing the protein in the A/California/7/2009 strain was incubated with a 5-fold molar excess of arbidol. This excess was to ensure complete or near complete binding of inhibitor to protein consistent with earlier studies (Swaminathan and Downard, 2012; Swaminathan et al., 2013). The protein–inhibitor complex was run on a native polyacrylamide gel aside a sample of the untreated protein. A separate stained band allowed for the blind excision of the gel piece containing protein–inhibitor complex and the protein alone to prevent denaturation. These were then each digested in-gel with endopro-

teinase Glu-C. Given that the antiviral inhibitor binding will shield the protease from accessing cleavage sites in its vicinity, a reduction in the relative levels of peptides recovered from the inhibitor binding site are expected.

The MALDI mass spectra recorded for the protein with and without arbidol are shown in Fig. 5. The identities of the major ions detected are shown in each spectrum. The spectra are very similar with the exception of a marked decrease in the relative abundance of the peptide ions at *m/z* 2109 (highlighted) associated with residues 448–464 of the full-length protein or residues 104–120 of the HA2 subunit.

The relative peak areas of all HA ions in both spectra are shown in Table 1. The difference in peak area differs by over 10%, the established experimental error in past studies (Kiselar and Downard, 1999; Morrissey and Downard, 2006; Morrissey et al., 2007; Schwahn and Downard, 2009; Swaminathan and Downard, 2012; Swaminathan et al., 2013), for only the peptide ions at *m/z* 2109. Although its peak area decreases by some 12% (absolute), the ion only has an initial relative area of 15% in the spectrum of the untreated protein and thus could not exceed this value in this case. The binding result was confirmed through application of an algorithm (PRISM) (Ho et al., 2007) developed to compare such spectral datasets unaided.

The full set of peptides detected in separate binding studies conducted using trypsin and chymotrypsin are shown in Fig. 6. Further confirmation for the binding of arbidol to a region of the HA2 subunit comes from the separate chymotryptic digest (data not shown). In this case, ions at *m/z* 1367.6244 corresponding to HA0 residues 453–463 (or HA2 residues 109–119) also undergo the largest change in relative area when spectra of the untreated and treated protein are considered. However, in this case the small relative area of the peak in the untreated hemagglutinin spectrum does not enable a confident prediction of binding. The same is true of tryptic peptide segment HA0 residues 451–460 (or HA2 107–116), where no tryptic peptides were found to bind to arbidol in a third binding experiment.

3.4. Mode of action – binding of arbidol to influenza hemagglutinin by molecular docking

To find further evidence of the binding of arbidol to influenza hemagglutinin, parallel molecular docking studies were performed. In this instance, the arbidol molecule was docked onto the HA2 subunit of a X-ray crystal structure of the protein using a published Xray crystal structure (3LZG). Consistent with a reported study (Leneva et al., 2009), the arbidol was found to bind in the vicinity of HA2 residues 118–123 in the high ranked results (rank 1 and 2). When bound in the vicinity of HA2 residues 118–123, in the stem region of the protein's structure, the arbidol molecule adopted two different orientations at approximately 180° to one another (Fig. 7).

Both the mass spectrometry and molecular docking results are consistent with a known arbidol resistance mutation K116R (residue 117 in the X-ray crystal structure) that resides within this peptide segment (Leneva et al., 2009).

4. Conclusions

The effect of arbidol on the proliferation of influenza virus *in vitro* through quantitation of hemagglutinin levels has been demonstrated using SDS–PAGE in conjugation mass spectrometric identification. An arbidol concentration of 20 μg/ml was required to achieve a 50% reduction in virus proliferation and hemagglutinin levels, a value consistent with a reported IC_{50} value for arbidol.

A MALDI mass spectrometry approach has identified residues HA2 subunit 104–120 of a H1 hemagglutinin that bind to arbidol and these results are in accord with parallel molecular docking results and reported resistant mutation data.

The combined studies support the recognized potential of arbidol as an effective and targeted antiviral agent against the influenza virus. Given the increasing resistance of strains of the virus to current antiviral inhibitors that target influenza neuraminidase, arbidol may have a greater future role in arresting and combating influenza infections.

Acknowledgements

The authors thank Mr. Robert Shaw and Dr. Ian Barr of the WHO Collaborating Centre for Reference and Research on Influenza for providing the clinical specimen used in this study. Z. Nasser and K. Downard thank Dr. Neil Fernandes for helpful guidance in the culturing of influenza virus stocks. K. Swaminathan is supported by a postgraduate scholarship funded by the Australian Research Council Discovery Project Grant (DP110101702) awarded to K. Downard.

References

Barry, J.M., 2006. The great influenza: the story of the deadliest pandemic in history. Penguin Books, New York.
Birnkrant, D., Cox, E., 2009. Emergency use authorization of peramivir. New Engl. J. Med. 361, 2204–2207.
Boriskin, Y.S., Leneve, I.A., Pecheur, E.I., et al., 2008. Arbidol, a broad-spectrum antiviral that blocks viral fusion. Curr. Med. Chem. 15, 997–1005.
Bouvier, N.M., Palese, P., 2008. The biology of influenza viruses. Vaccine 26, D49–53.
Couch, R.B., 2000. Prevention and treatment of influenza. New Engl. J. Med. 343, 1778–1787.
Fanning, T.G., Taubenberger, J.K., 1999. Phylogenetically important regions of the influenza A H1 hemagglutinin protein. Virus Res. 65, 33–42.
Gamblin, S.J., Haire, L.F., Russell, R.J., Stevens, D.J., Xiao, B., Ha, Y., Vasisht, N., Steinhauer, D.A., Daniels, R.S., Elliot, A., Wiley, D.C., Skehel, J.J., 2004. The structure and receptor binding properties of the 1918 influenza hemagglutinin. Science 303, 1838–1842.
Hampson, A.W., Mackenzie, J.S., 2006. The influenza viruses. Med. J. Aust. 185, S39–S43.
Hauge, S.H., Dudman, S., Borgen, K., Lackenby, A., Hungnes, O., 2009. Oseltamivir-resistant influenza viruses A (H1N1), Norway, 2007–2008. Emerg. Infect. Dis. 15, 155–162.
Ho, J.W.K., Morrissey, B., Downard, K.M., 2007. A computer algorithm for the identification of protein interactions from the spectra of masses (PRISM). J. Am. Soc. Mass Spectrom. 18, 563–566.
Hurt, A.C., Holien, J.K., Parker, M.W., Barr, I.G., 2009. Oseltamivir resistance and the H274Y neuraminidase mutation. Drugs 69, 2523–2531.
Kilbourne, E.D., 2006. Influenza pandemics of the 20th century. Emerg. Infectious Dis. 12, 9–14.
Kiselar, J.G., Downard, K.M., 1999. Antigenic surveillance of the influenza virus by mass spectrometry. Biochemistry 43, 14185–14191.
Leneva, I.A., Fadeeva, N.I., Fedyakina, I.T., 1994. The study of effect of a new antiviral drug arbidol on different stages of viral reproduction. Antiviral Res. 23, 187–199.
Leneva, I.A., Russell, R.J., Boriskin, Y.S., et al., 2009. Characteristics of arbidol-resistant mutants of influenza virus: implications for the mechanism of anti-influenza action of arbidol. Antiviral Res. 81, 132–140.
Li, C., Shao, M., Cui, X., Song, Y., et al., 2010. Application of deglycosylation and electrophoresis to the quantification of influenza viral hemagglutinins facilitating the production of 2009 pandemic influenza (H1N1) vaccines at multiple manufacturing sites in China. Biologicals 38, 284–289.
Morrissey, B., Downard, K.M., 2006. A proteomics approach to survey the antigenicity of the influenza virus by mass spectrometry. Proteomics 6, 2034–2041.
Morrissey, B., Streamer, M., Downard, K.M., 2007. Antigenic characterisation of H3N2 subtypes of the influenza virus by mass spectrometry. J. Virol. Methods 145, 106–114.
Moscona, A., 2005. Neuraminidase inhibitors for influenza. New Engl. J. Med. 353, 1363–1373.
Moscona, A., 2009. Global transmission of oseltamivir-resistant influenza. N. Engl. J. Med. 360, 953–956.
Pereira, M.S., 1980. The effects of shifts and drifts on the epidemiology of influenza in man. Phil. Trans. Royal Soc. Lond. Biol. Sci. 288, 423–432.
Poland, G.A., Rottinghaus, S.T., Jacobson, R.M., 2001. Influenza vaccines: a review and rationale for use in developed and underdeveloped countries. Vaccine 19, 2216–2220.

Schwahn, A.B., Downard, K.M., 2009. Antigenicity of a type A influenza virus through comparison of hemagglutination inhibition and mass spectrometry immunoassays. J. Immunoassay Immunochem. 30, 245–261.
Shi, L., Xiong, H., He, J., et al., 2007. Antiviral activity of arbidol against influenza A virus, respiratory syncytial virus, rhinovirus, coxsackie virus and adenovirus *in vitro* and *in vivo*. Arch. Virol. 152, 1447–1455.
Subbarao, K., Katz, J., 2000. Avian influenza viruses infecting humans. Cell. Mol. Life Sci. 57, 1770–1784.
Swaminathan, K., Downard, K.M., 2012. Anti-viral inhibitor binding to influenza neuraminidase by MALDI mass spectrometry. Anal. Chem. 84, 3725–3730.
Swaminathan, K., Dyason, J.C., Maggioni, A., et al., 2013. Binding of a natural anthocyanin inhibitor to influenza neuraminidase by mass spectrometry. Anal. Bioanal. Chem. 405, 6563–6572.
Vavricka, C.J., Li, Q., Wu, Y., Qi, J., et al., 2011. Structural and functional analysis of laninamivir. PLoS Pathog. 7, e1002249.
Von Itzstein, M., Thomson, R., 2009. Anti-influenza drugs: the development of sialidase inhibitors. Handb. Exp. Pharmacol. 189, 111–154.
Wilschut, J., Mcelhaney, J., Palache, A., 2006. Rapid Reference to Influenza, second ed. Mosby-Elsevier, Netherlands.
World Health Organization, 2009. Influenza fact sheet No. 211, http://www.who.int/mediacentre/factsheets/fs211/en/.
World Health Organization,2010, Oseltamivir resistance, Weekly Update (August).